

# Investigation of Proton-Proton Short-Range Correlations via the $^{12}\text{C}(e,e'pp)$ Reaction

R. Shneur,<sup>1</sup> P. Monaghan,<sup>2</sup> R. Subedi,<sup>3</sup> B. D. Anderson,<sup>3</sup> K. Aniol,<sup>4</sup> J. Annand,<sup>5</sup> J. Arrington,<sup>6</sup> H. Benaoum,<sup>7</sup> F. Benmokhtar,<sup>8</sup> P. Bertin,<sup>9</sup> W. Bertozzi,<sup>2</sup> W. Boeglin,<sup>10</sup> J. P. Chen,<sup>11</sup> Seonho Choi,<sup>12</sup> E. Chudakov,<sup>11</sup> E. Cisbani,<sup>13</sup> B. Craver,<sup>14</sup> C. W. de Jager,<sup>11</sup> R. Feuerbach,<sup>11</sup> S. Frullani,<sup>13</sup> F. Garibaldi,<sup>13</sup> O. Gayou,<sup>2</sup> S. Gilad,<sup>2</sup> R. Gilman,<sup>15,11</sup> O. Glamazdin,<sup>16</sup> J. Gomez,<sup>11</sup> O. Hansen,<sup>11</sup> D. W. Higinbotham,<sup>11</sup> T. Holmstrom,<sup>17</sup> H. Ibrahim,<sup>18</sup> R. Igarashi,<sup>19</sup> E. Jans,<sup>20</sup> X. Jiang,<sup>15</sup> Y. Jiang,<sup>21</sup> L. Kaufman,<sup>22</sup> A. Kelleher,<sup>17</sup> A. Kolarkar,<sup>23</sup> E. Kuchina,<sup>15</sup> G. Kumbartzki,<sup>15</sup> J. J. LeRose,<sup>11</sup> R. Lindgren,<sup>14</sup> N. Liyanage,<sup>14</sup> D. J. Margaziotis,<sup>4</sup> P. Markowitz,<sup>10</sup> S. Marrone,<sup>13</sup> M. Mazouz,<sup>24</sup> R. Michaels,<sup>11</sup> B. Moffit,<sup>17</sup> S. Nanda,<sup>11</sup> C. F. Perdrisat,<sup>17</sup> E. Piassetzky,<sup>1</sup> M. Potokar,<sup>25</sup> V. Punjabi,<sup>26</sup> Y. Qiang,<sup>2</sup> J. Reinhold,<sup>10</sup> B. Reitz,<sup>11</sup> G. Ron,<sup>1</sup> G. Rosner,<sup>5</sup> A. Saha,<sup>11</sup> B. Sawatzky,<sup>14,27</sup> A. Shahinyan,<sup>28</sup> S. Širca,<sup>25,29</sup> K. Slifer,<sup>14,27</sup> P. Solvignon,<sup>27</sup> V. Sulkosky,<sup>17</sup> N. Thompson,<sup>5</sup> P. E. Ulmer,<sup>18</sup> G. M. Urciuoli,<sup>13</sup> E. Voutier,<sup>24</sup> K. Wang,<sup>14</sup> J. W. Watson,<sup>3</sup> L.B. Weinstein,<sup>18</sup> B. Wojtsekhowski,<sup>11</sup> S. Wood,<sup>11</sup> H. Yao,<sup>27</sup> X. Zheng,<sup>6,2</sup> and L. Zhu<sup>30</sup>

(The Jefferson Lab Hall A Collaboration)

<sup>1</sup>Tel Aviv University, Tel Aviv 69978, Israel

<sup>2</sup>Massachusetts Institute of Technology, Cambridge, Massachusetts 02139, USA

<sup>3</sup>Kent State University, Kent, Ohio 44242, USA

<sup>4</sup>California State University Los Angeles, Los Angeles, California 90032, USA

<sup>5</sup>University of Glasgow, Glasgow G12 8QQ, Scotland, UK

<sup>6</sup>Argonne National Laboratory, Argonne, Illinois, 60439, USA

<sup>7</sup>Syracuse University, Syracuse, New York 13244, USA

<sup>8</sup>University of Maryland, College Park. Maryland 20742, USA

<sup>9</sup>Laboratoire de Physique Corpusculaire, F-63177 Aubièrre, France

<sup>10</sup>Florida International University, Miami, Florida 33199, USA

<sup>11</sup>Thomas Jefferson National Accelerator Facility, Newport News, Virginia 23606, USA

<sup>12</sup>Seoul National University, Seoul 151-747, Korea

<sup>13</sup>INFN, Sezione Sanità and Istituto Superiore di Sanità, Laboratorio di Fisica, I-00161 Rome, Italy

<sup>14</sup>University of Virginia, Charlottesville, Virginia 22904, USA

<sup>15</sup>Rutgers, The State University of New Jersey, Piscataway, New Jersey 08855, USA

<sup>16</sup>Kharkov Institute of Physics and Technology, Kharkov 310108, Ukraine

<sup>17</sup>College of William and Mary, Williamsburg, Virginia 23187, USA

<sup>18</sup>Old Dominion University, Norfolk, Virginia 23508, USA

<sup>19</sup>University of Saskatchewan, Saskatoon, Saskatchewan, Canada S7N 5E2

<sup>20</sup>Nationaal Instituut voor Kernfysica en Hoge-Energiefysica, Amsterdam, The Netherlands

<sup>21</sup>University of Science and Technology of China, Hefei, Anhui, China

<sup>22</sup>University of Massachusetts Amherst, Amherst, Massachusetts 01003, USA

<sup>23</sup>University of Kentucky, Lexington, Kentucky 40506, USA

<sup>24</sup>Laboratoire de Physique Subatomique et de Cosmologie, 38026 Grenoble, France

<sup>25</sup>Institute "Jožef Stefan", 1000 Ljubljana, Slovenia

<sup>26</sup>Norfolk State University, Norfolk, Virginia 23504, USA

<sup>27</sup>Temple University, Philadelphia, Pennsylvania 19122, USA

<sup>28</sup>Yerevan Physics Institute, Yerevan 375036, Armenia

<sup>29</sup>Dept. of Physics, University of Ljubljana, 1000 Ljubljana, Slovenia

<sup>30</sup>University of Illinois at Urbana-Champaign, Urbana, Illinois 61801, USA

(Dated: October 30, 2018)

We investigated simultaneously the  $^{12}\text{C}(e,e'p)$  and  $^{12}\text{C}(e,e'pp)$  reactions at  $Q^2 = 2$  (GeV/c)<sup>2</sup>,  $x_B = 1.2$ , and in an  $(e,e'p)$  missing-momentum range from 300 to 600 MeV/c. At these kinematics, with a missing-momentum greater than the Fermi momentum of nucleons in a nucleus and far from the delta excitation, short-range nucleon-nucleon correlations are predicted to dominate the reaction. For  $(9.5 \pm 2)\%$  of the  $^{12}\text{C}(e,e'p)$  events, a recoiling partner proton was observed back-to-back to the  $^{12}\text{C}(e,e'p)$  missing momentum vector, an experimental signature of correlations.

PACS numbers: 21.60.-n, 24.10.-i, 25.30.-c

The short-range component of the nucleon-nucleon force manifests itself via nucleon pairs inside a nucleus. Such nucleon pairs have a low center-of-mass momentum and a high relative momentum [1] where low and high are relative to the Fermi sea level,  $k_F$ , which for  $^{12}\text{C}$  is

$\sim 220$  MeV/c [2]. We refer to such a proton pair as a proton-proton short-range correlation (pp-SRC). Averaged over all nucleon momenta, the probability for a nucleon in  $^{12}\text{C}$  to be a member of a two-nucleon SRC state, proton-proton (pp), proton-neutron (pn), or neutron-

neutron (nn), has been estimated from the dependence of inclusive (e,e') data on the Bjorken scaling variable,  $x_B$ , to be  $20 \pm 5\%$  [3, 4, 5]. Measurements at Brookhaven National Laboratory (BNL) of (p,pp) and (p,ppn) at high momentum transfer [6, 7, 8] verified the existence of correlated np pairs; subsequent analysis of these data set an upper limit of 3% for pp-SRCs in  $^{12}\text{C}$  [9].

Even though the probability of pp-SRCs in nuclei is small, they are important since they can teach us about the strong interaction at short distances. Moreover, as a manifestation of asymmetric dense cold nuclear matter that can be studied in the laboratory, they are relevant to the understanding of neutron stars [10].

In this work, we determine the fraction of  $^{12}\text{C}(e,e'p)$  events which are associated with pp-SRC pairs. This was done by measuring the ratio of the  $^{12}\text{C}(e,e'pp)$  and the  $^{12}\text{C}(e,e'p)$  cross sections as a function of the (e,e'p) missing momentum,  $p_{miss}$ , where  $\vec{p}_{miss} = \vec{p} - \vec{q}$  as shown in Fig. 1. By measuring above the Fermi sea of nucleon motion, i.e. greater than 220 MeV/c, and in kinematics where other reaction mechanisms are suppressed, if the initial struck nucleon is part of a pair, one would expect a single recoil nucleon to balance the missing momentum vector. In the impulse approximation, a virtual photon with a large  $Q^2$  is absorbed by one of the protons in the pair. This supplies the energy required to break the pair and remove the two protons from the nucleus. Pre-existing pairs are identified by detecting a recoiling proton in coincidence with an (e,e'p) event, where the recoiling proton has a high momentum ( $\vec{p}_{rec}$ ) opposite to the direction but of roughly equal magnitude to  $\vec{p}_{miss}$  (see Fig. 1).

Historically, the interpretation of triple-coincidence data in terms of SRCs has been plagued by contributions from meson-exchange currents (MECs), isobar configurations (ICs) and final-state interactions (FSIs) [11, 12, 13]. The kinematics for the measurements described here were chosen to minimize these effects. For example, at high  $Q^2$ , MEC contributions decrease as  $1/Q^2$  relative to PWIA contributions and are reduced relative to those due to SRC [14, 15]. A large  $Q^2$  and  $x_B$  also drastically reduces IC contributions [16, 17]. Finally, FSIs are minimized by having a large  $\vec{p}_{miss}$  component antiparallel to the virtual photon direction [16].

This experiment was performed in Hall A of the Thomas Jefferson National Accelerator Facility (JLab) using an incident electron beam of 4.627 GeV with a current between 5 and 40  $\mu\text{A}$ . The target was a 0.25 mm thick graphite sheet rotated  $70^\circ$  from perpendicular to the beam line to minimize the material through which the recoiling protons passed. The two Hall A high-resolution spectrometers (HRS) [18] were used to identify the  $^{12}\text{C}(e,e'p)$  reaction. Scattered electrons were detected in the left HRS (HRS-L) at a central scattering angle (momentum) of  $19.5^\circ$  (3.724 GeV/c). This corresponds to the quasi-free knockout of a single pro-

ton with transferred three-momentum  $|\vec{q}| = 1.65 \text{ GeV}/c$ , transferred energy  $\omega = 0.865 \text{ GeV}$ ,  $Q^2 = 2 \text{ (GeV}/c)^2$ , and  $x_B \equiv \frac{Q^2}{2m\omega} = 1.2$  where  $m$  is the mass of a proton. Knocked-out protons were detected using the right HRS (HRS-R) which was set at 3 different combinations of central angle and momentum:  $40.1^\circ$  & 1.45 GeV/c,  $35.8^\circ$  & 1.42 GeV/c, and  $32.0^\circ$  & 1.36 GeV/c. These kinematic settings correspond to median missing-momentum values  $p_{miss} = 0.35, 0.45$  and  $0.55 \text{ GeV}/c$ , respectively, with a range of approximately  $\pm 50 \text{ MeV}/c$  each.

A third, large-acceptance spectrometer, BigBite, was used to detect recoiling protons in the  $^{12}\text{C}(e,e'pp)$  events. The BigBite spectrometer [19] consists of a large-acceptance, non-focusing dipole magnet and a detector package. For this measurement, the magnet was located at an angle of  $99^\circ$  and 1.1 m from the target with a resulting angular acceptance of about 96 msr and a nominal momentum acceptance from 0.25 GeV/c to 0.9 GeV/c. The detector package was constructed specifically for this experiment. It consisted of three planes of plastic scintillator segmented in the dispersive direction. The first scintillator plane (the "auxiliary plane"), was placed at the exit of the dipole, parallel to the magnetic field boundary, and consisted of 56 narrow scintillator bars of dimension  $350 \times 25 \times 2.5 \text{ mm}^3$ . The second and third scintillator planes, known collectively as the trigger plane, were mounted together and were located 1 meter downstream of the first plane. The second and third planes consisted of 24 scintillator bars each, with dimensions  $500 \times 86 \times 3 \text{ mm}^3$  and  $500 \times 86 \times 30 \text{ mm}^3$ , respectively. The scintillator bars in these two layers were offset from one another by half a bar in the dispersive direction, improving their position resolution by a factor of two. Each of the scintillator bars in the auxiliary plane was read out by one photomultiplier tube (PMT), while each of the trigger scintillators was read out by two PMTs, one on each end. This unshielded system was able to run in Hall A up to a luminosity of  $10^{38} \text{ cm}^{-2}\text{s}^{-1}$  per nucleon.

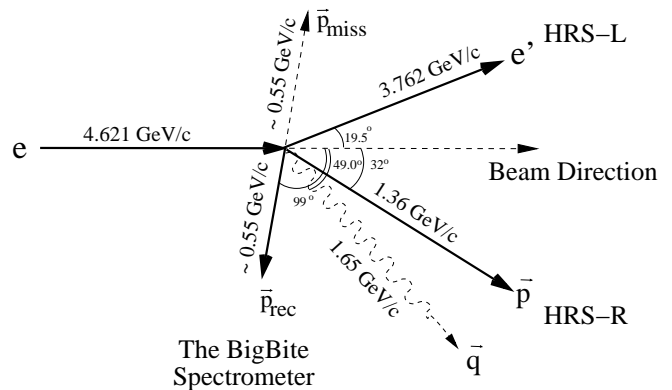


FIG. 1: A vector diagram of the layout of the  $^{12}\text{C}(e,e'pp)$  experiment shown for the largest  $p_{miss}$  kinematics of 0.55 GeV/c.

The coincident  $^{12}\text{C}(e,e'p)$  events were detected in the two HRSs, with a typical trigger rate of 0.2 Hz. After spectrometer acceptance cuts, the time-difference distribution showed a clear electron-proton coincidence peak with a width of  $\sim 0.5$  ns sigma. The measured  $^{12}\text{C}(e,e'p)$  missing-energy spectrum for the lowest missing-momentum setting ( $p_{\text{miss}} \sim 0.35$  GeV/c) is shown in Fig. 2. Missing energy is defined by  $E_{\text{miss}} \equiv \omega - T_p - T_{A-1}$ , where  $T_p$  is the measured kinetic energy of the knocked-out proton and  $T_{A-1}$  is the calculated kinetic energy of the residual A-1 system. The contribution of missing energy due to a single proton removal from the  $p$ -shell in  $^{12}\text{C}$ , leaving the  $^{11}\text{B}$  nucleus in its ground state, is seen as a peak at missing energy of about 16 MeV. The strength above the  $^{11}\text{B}$  ground state is comprised of  $p$ -shell removal to highly-excited bound states and  $p$ -shell and  $s$ -shell removal to the continuum. The contribution due to  $\Delta$ -resonance excitation was removed by requiring  $\vec{p}_{\text{miss}}$  to point in the direction one would expect from the break-up of a pair, e.g.  $< 76^\circ$ ,  $< 84^\circ$ , and  $< 88^\circ$  for the three kinematics, respectively. This cut removes the  $\Delta$ -resonance, since the missing-momentum vector for pion production events by conservation of energy and momentum points to larger angles than direct knock-out events. The measured missing-energy spectrum with and without this angular cut is shown in Fig. 2.

The BigBite spectrometer was positioned to determine if a single high-momentum proton was balancing the  $p_{\text{miss}}$  of the  $(e,e'p)$  reaction. Such recoiling protons were identified in BigBite using the measured energy loss in the scintillator detectors and the consistency between the measured time-of-flight (TOF) and the momentum measured by the trajectory in the magnetic field. The momentum resolution of BigBite, determined from elastic electron-proton scattering, was  $\frac{\Delta p}{p} = 4\%$ . The singles rates with a  $30 \mu\text{A}$  beam were about 100 kHz per scintillator in the first plane and 80 kHz per scintillator in the third plane. With these rates, nearly all events had only one track with a reconstructed momentum consistent with the momentum from the TOF. For the small number of events that had more than one possible reconstructed track, we selected the track that had the most consistent momentum between the TOF determination and from ray tracing. Primarily due to the gaps between scintillators, the overall proton detection efficiency was 85%.

The TOF for protons detected in BigBite was defined from the target to the third scintillator plane ( $\sim 3$  m) assuming the protons leave the center of the target at the same time as the scattered electrons and the knocked-out protons and was corrected using the reconstructed trajectory path length. The timing peak shown in the insert of Fig. 2 is thus due to real triple coincidences and the flat background is due to random coincidences between the  $^{12}\text{C}(e,e'p)$  reaction and protons in BigBite. The use of a proton identification cut, an angular acceptance cut

in BigBite, and a TOF cut of  $\pm 3.5$  ns to select the real coincidences, resulted in signal/background ratios of 1:2, 1:1, and 2:1 for the median missing-momentum settings of 0.35, 0.45 and 0.55 GeV/c, respectively.

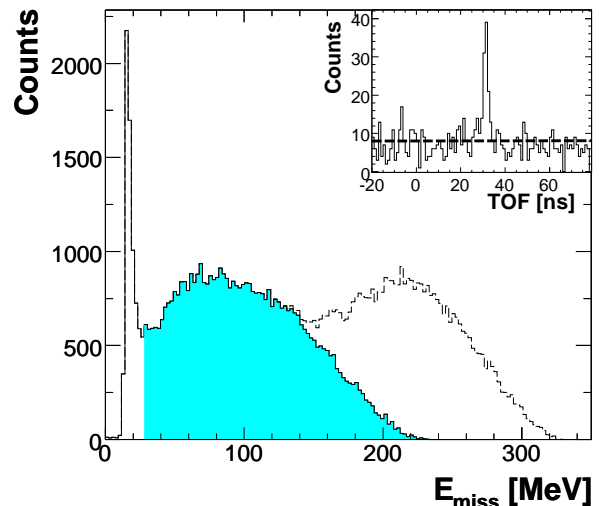


FIG. 2: The measured  $^{12}\text{C}(e,e'p)$  missing-energy spectrum for  $p_{\text{miss}} \sim 0.31$  GeV/c. The peak at 16 MeV is due to removal of  $p$ -shell protons leaving the  $^{11}\text{B}$  in its ground state. The shaded region contains events with residual excited bound or continuum states. The dashed line contains events in which the  $\Delta$  was excited. Inserted is the TOF spectrum for protons detected in BigBite in coincidence with the  $^{12}\text{C}(e,e'p)$  reaction. The random background is shown as a dashed line.

For the highest  $p_{\text{miss}}$  setting, Fig. 3 shows the cosine of the angle,  $\gamma$ , between the missing momentum ( $\vec{p}_{\text{miss}}$ ) and the recoiling proton detected in BigBite ( $\vec{p}_{\text{rec}}$ ). We also show in Fig. 3 the angular correlation for the random background as defined by a time window off the coincidence peak. The back-to-back peak of the real triple coincidence events is demonstrated clearly. The curve is a result of a simulation of the scattering off a moving pair having a center-of-mass (c.m.) momentum width of 0.136 GeV/c as discussed below. Similar back-to-back correlations were observed for the other kinematic settings.

In the plane-wave impulse approximation (PWIA) the c.m. momentum of a pp-SRC pair is given by:

$$\vec{p}_{c.m.} \equiv \vec{p}_{\text{miss}} + \vec{p}_{\text{rec}}. \quad (1)$$

For the triple-coincident events, we reconstructed the two components of  $\vec{p}_{c.m.}$  in the direction towards BigBite and vertical to the scattering plane. In these directions the acceptance was large enough to be sensitive to the magnitude of the c.m. motion.

To avoid distortions due to the finite acceptance of BigBite, we compared the measured distributions of these components to simulated distributions that were pro-

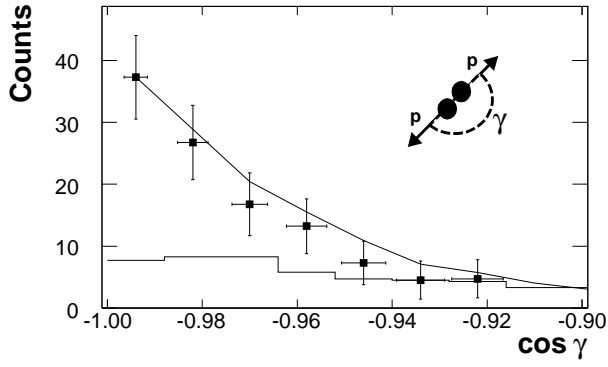


FIG. 3: The distribution of the cosine of the opening angle between the  $\vec{p}_{miss}$  and  $\vec{p}_{rec}$  for the  $p_{miss} = 0.55$  GeV/c kinematics. The histogram shows the distribution of random events. The curve is a simulation of the scattering off a moving pair with a width of 0.136 GeV/c for the pair c.m. momentum.

duced using MCEEP [20]. The finite angular and momentum acceptances of BigBite were modeled in the simulation by applying the same cuts on the recoiling protons as were applied to the data. The simulations assume that an electron scatters off a moving pp pair with a c.m. momentum relative to the A-2 spectator system described by a Gaussian distribution, as in [21]. We assumed an isotropic 3-dimensional motion of the pair and varied the width of the Gaussian motion equally in each direction until the best agreement with the data was obtained. The six measured distributions (two components in each of the three kinematic settings) yield, within uncertainties, the same width with a weighted average of  $0.136 \pm 0.020$  GeV/c. This width is consistent with the width determined from the (p,ppn) experiment at BNL [7], which was  $0.143 \pm 0.017$  GeV/c. It is also in agreement with the theoretical prediction of 0.139 GeV/c in reference [21].

The measured ratio of  $^{12}\text{C}(e,e'pp)$  to  $^{12}\text{C}(e,e'p)$  events is given by the ratio of events in the background-subtracted TOF peak (insert in Fig. 2) to those in the shaded area in the  $E_{miss}$  spectrum of Fig. 2. This ratio, as a function of  $p_{miss}$  in the  $^{12}\text{C}(e,e'p)$  reaction, is shown as the full squares in the upper panel of Fig. 4. The uncertainties are dominated by statistical errors; the uncertainty in separating out events from  $\Delta$ -production is small.

The measured ratio can be translated to the ratio of the nine-fold differential cross section for the  $^{12}\text{C}(e,e'pp)$  reaction to the six-fold differential cross section for the  $^{12}\text{C}(e,e'p)$  reaction. This ratio is presented as the open squares in Fig. 4. For simplicity, the error bars on the differential cross sections ratios are not shown because they are very similar to those of the yield ratios.

The measured ratios in the upper panel of Fig. 4 are limited by the finite acceptance of BigBite. We used

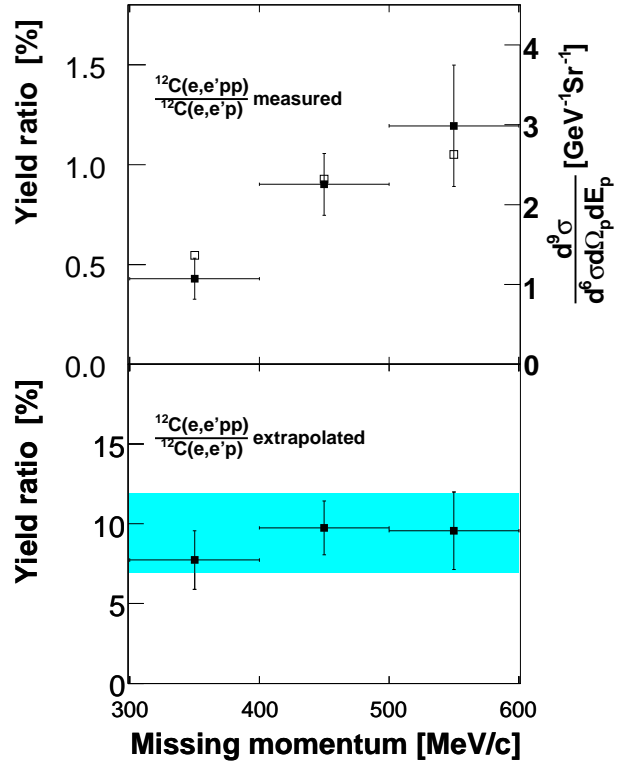


FIG. 4: The measured and extrapolated ratios of yields for the  $^{12}\text{C}(e,e'pp)$  and the  $^{12}\text{C}(e,e'p)$  reactions. The full squares are the yield ratios and the open squares are the corresponding ratios of the differential cross sections for the  $^{12}\text{C}(e,e'pp)$  reaction to the  $^{12}\text{C}(e,e'p)$  reaction. A simulation was used to account for the finite acceptance of BigBite and make the extrapolation to the total number of recoiling proton pairs shown in lower figure. The gray area represents a band of  $\pm 2\sigma$  uncertainty in the width of the c.m. momentum of the pair.

the simulation described above to account for this finite acceptance; the resulting extrapolated ratios are shown in the lower panel of Fig. 4. The simulation used a Gaussian distribution (of width 0.136 GeV/c as determined above) for the c.m. momentum of the pp pairs. The shaded band in the figure corresponds to using a width  $\pm 0.040$  GeV/c (two standard deviations). From this result, we conclude that in the  $p_{miss}$  range between 0.30 and 0.60 GeV/c,  $(9.5 \pm 2)\%$  of the  $^{12}\text{C}(e,e'p)$  events have a second proton that is ejected roughly back-to-back to the first one, with very little dependence on  $p_{miss}$ .

While the detected protons are correlated in time, effects other than pp-SRC, such as FSI, can cause the correlation. In fact, FSIs can occur between protons in a pp-SRC pair as well as with the other nucleons in the residual A-2 system. Interactions between nucleons in a pair conserve the isospin structure of the pair (i.e. pp pairs remain pp pairs). Elastic FSIs between members of the SRC pair also do not change the c.m. momentum

of the pair as reconstructed from the momentum of the detected particles.

The elastic (real) part of the FSI with the A-2 nucleons can alter the momenta, such as to make  $\vec{p}_{miss}$  and/or  $\vec{p}_{rec}$  and hence  $\vec{p}_{c.m.}$  different from Eqn. 1. The absorptive (imaginary) part of the FSI can reduce the  $^{12}\text{C}(e,e'pp)/^{12}\text{C}(e,e'p)$  ratio, while single charge exchange can turn pn-SRC pairs into  $^{12}\text{C}(e,e'pp)$  events, thereby increasing the measured ratio. Our estimates of these FSI effects, based on a Glauber approximation using the method described in [22], indicate that the absorption and single charge exchange compensate each other so that the net effect is small compared to the uncertainties in the measurement. This conclusion is backed by the c.m. motion result which gives widths for all the components that are narrow and internally consistent.

In summary, we measured simultaneously the  $^{12}\text{C}(e,e'p)$  and  $^{12}\text{C}(e,e'pp)$  reactions in kinematics designed to maximize observation of SRCs while suppressing other effects such as FSIs, ICs, and MECs. We identified directionally-correlated proton pairs in  $^{12}\text{C}$  using the  $^{12}\text{C}(e,e'pp)$  reaction and determined the fraction of the  $^{12}\text{C}(e,e'p)$  events at large  $p_{miss}$  from pp-SRCs to be  $(9.5 \pm 2)\%$ . In the PWIA, the c.m. momentum distribution of the  $pp$ -SRC pair was determined to have a Gaussian shape with a width of  $0.136 \pm 0.020$  GeV/c.

We would like to acknowledge the contribution of the Hall A collaboration and technical staff. Useful discussions with J. Alster, C. Ciofi degli Atti, the late K. Egiyan, A. Gal, L. Frankfurt, J. Ryckebusch, M. Strikman, and M. Sargsian, are gratefully acknowledged. This work was supported by the Israel Science Foundation, the US-Israeli Bi-national Scientific Foundation, the UK Engineering and Physical Sciences Research Council, the U.S. National Science Foundation, the U.S. Department of Energy grants DE-AC02-06CH11357, DE-FG02-94ER40818, and U.S. DOE Contract No. DE-AC05-

84150, Modification No. M175, under which the South-eastern Universities Research Association, Inc. operates the Thomas Jefferson National Accelerator Facility.

- 
- [1] L. L. Frankfurt and M. I. Strikman, Phys. Rept. **76** (1981).
  - [2] E. J. Moniz et al., Phys. Rev. Lett. **26**, 445 (1971).
  - [3] L. L. Frankfurt, M. I. Strikman, D. B. Day, and M. Sargsian, Phys. Rev. **C48**, 2451 (1993).
  - [4] K. S. Egiyan et al. (CLAS), Phys. Rev. **C68**, 014313 (2003).
  - [5] K. S. Egiyan et al. (CLAS), Phys. Rev. Lett. **96**, 082501 (2006).
  - [6] J. L. S. Aclander et al., Phys. Lett. **B453**, 211 (1999).
  - [7] A. Tang et al., Phys. Rev. Lett. **90**, 042301 (2003).
  - [8] A. Malki et al., Phys. Rev. **C65**, 015207 (2002).
  - [9] E. Piassetzky, M. Sargsian, L. Frankfurt, M. Strikman, and J. W. Watson, Phys. Rev. Lett. **97**, 162504 (2006).
  - [10] M. M. Sargsian et al., J. Phys. **G29**, R1 (2003).
  - [11] L. J. H. M. Kester et al., Phys. Rev. Lett. **74**, 1712 (1995).
  - [12] K. I. Blomqvist et al., Phys. Lett. **B421**, 71 (1998).
  - [13] D. L. Groep et al., Phys. Rev. **C63**, 014005 (2001).
  - [14] R. G. Arnold et al., Phys. Rev. **C42**, 1 (1990).
  - [15] J. M. Laget, Phys. Lett. **B199**, 493 (1987).
  - [16] L. L. Frankfurt, M. M. Sargsian, and M. I. Strikman, Phys. Rev. **C56**, 1124 (1997).
  - [17] M. M. Sargsian, Int. J. Mod. Phys. **E10**, 405 (2001).
  - [18] J. Alcorn et al., Nucl. Instrum. Meth. **A522**, 294 (2004).
  - [19] D. W. Higinbotham et al., to be submitted to Nucl. Instrum. Meth. (2007).
  - [20] P. Ulmer et al., *MCEEP: Monte carlo for (e,e'p) experiments* (2006).
  - [21] C. Ciofi degli Atti and S. Simula, Phys. Rev. **C53**, 1689 (1996).
  - [22] I. Mardor, Y. Mardor, E. Piassetzky, J. Alster, and M. M. Sargsian, Phys. Rev. **C46**, 761 (1992).